CHEMICAL REACTIVITY AND THE STRUCTURE OF GELS (*)

by C.J. BRINKER and B.C. BUNKER (1), D.R. TALLANT and K.J. WARD (2)

(1) Inorganic Materials Chemistry, Division 1846.
(2) Surface Chemistry and Analysis, Division 1823.
Sandia National Laboratories, Albuquerque, NM 87185 USA.

ABSTRACT

The structures of sel-gel-derived networks are a product of a series of condensation reactions. In solution, the evolving structures are limited to species which are stable in the synthesis medium (alcohol/water). During consolidation metastable species form, which are temporarily stabilized by the high viscosity of the surrounding matrix. Chemical reactivity of gel-derived networks provides insight to their structure and vice versa.
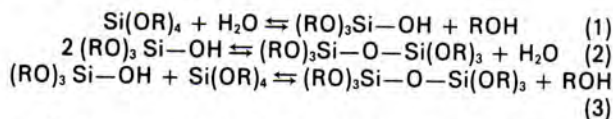
RÉSUMÉ

La structure des réseaux obtenus par le procédé sol-gel est dérivée d'une série de réactions de condensation. Les seules structures qui se dégagent en solution sont celles qui sont stables dans l'entourage de synthèse (alcool/eau). Des espèces métastables formées lors de la consolidation sont stabilisées temporairement par la viscosité élevée de la matrice environnante. La réactibilité chimique des réseaux sol-gels permet de clarifier leur structure et vice versa.

Introduction

I.1. Sol-Gel Processing

The sol-gel process of glass formation uses metal alkoxides of network forming elements (e.g., $M(OR)_x$, where M is Si, B, Ti, Al, etc., and R is often an alkyl group) as monomeric glass precursors. In alcohol/water solutions the alkoxide groups are removed stepwise by acid or base catalyzed hydrolysis reactions and are replaced by hydroxyl groups (Eq. 1). Subsequent condensation reactions involving the hydroxyl groups yield polymeric solution species composed of M-O-M linkages (Eqs. 2 and 3). It should be noted that, although Eqs. 1-3 (in the forward direction) are used generically to describe gelation, these reactions are more or less reversible depending on pH, water concentration, temperature etc. and in addition depend on the connectivity of M from the standpoint of steric, inductive, and structural considerations.

$$Si(OR)_4 + H_2O \rightleftharpoons (RO)_3Si-OH + ROH \quad (1)$$
$$2 (RO)_3 Si-OH \rightleftharpoons (RO)_3Si-O-Si(OR)_3 + H_2O \quad (2)$$
$$(RO)_3 Si-OH + Si(OR)_4 \rightleftharpoons (RO)_3Si-O-Si(OR)_3 + ROH \quad (3)$$

When the polymerization process is extensive, the system gels. At the gel point physical properties such as viscosity and elastic modulus diverge, freezing-in the solution structure. Structural alterations continue, however, as the solvent is evaporated to form a porous xerogel. This drying process results in a compaction of the original solution structure, allowing condensation reactions to continue as reactive silanol groups encounter one another. Xerogels are characteristically high surface area materials (surface areas = 100 to 1 200 m²/g). Thermal treatments between 500 and 1 000 °C are generally employed for their consolidation (see, e.g., refs. 1-3).

I.2. Structural Evolution

In order to form gels, the successive series of hydrolysis, condensation, and restructuring (reverse of Eqs. 1-3) steps must result in infinite networks which are stable in the solution medium (typically alcohol/water). However during the drying and consolidation steps the structure continues to evolve via polycondensation mostly in the absence of solvent. Thus structural evolution in gel-derived glasses occurs in two stages. Initially in solution the polymeric structure is readily modified by reactions with the solvent and/or condensation products. Hence the structure of gels and desiccated porous xerogels is composed principally of stable solution species. During consolidation, condensation reactions continue to occur under relatively inert conditions at temperatures much less than the T_g of the conventionally melted glass. Structures formed during this stage reflect the products of condensation reactions which, due to the enormously high viscosity and relative absence of reactive environmental molecules, have been unable to undergo restructuring. During the final stage of consolidation $(T \rightarrow T_g)$, structural rearrangements are made possible by the reduced viscosity.

Structural evolution in gel-derived glasses is therefore distinctly different from that in melt-prepared glasses. Whereas the structure of melt-prepared glass largely reflects the thermodynamic conditions imposed during high temperature melting and annealing followed by *cooling* toward T_g the structure of gel-derived glasses (although initially "frozen-in" during gelation) continues to evolve as a product of condensation reactions which occur during *heating* toward the conventional T_g, at temperatures where the viscosity is in excess of 10^{13} poises [2,3]. This distinction, i.e. approaching T_g from above versus from below, requires the structures of melt-prepared glasses to be very near equilibrium (relaxation times at $T > T_g$ are a few seconds) [4], while

metastable structures, which conceivably form as products of condensation reactions, may persist in gels which are processed at low temperatures where the viscosity is enormous and relaxation times are significantly lengthened ($> 10^6$ s) ([4]).

This paper reviews recent information we have obtained concerning : 1) the structure of gels and the influence of structure on chemical reactivity; and 2) the manner in which chemical reactivity influences the structure of gels. Two chemically and structurally dissimilar gel systems are discussed : pure silica and lithium borates ($x\text{Li}_2\text{O} \cdot (1-x)\text{B}_2\text{O}_3$; where $x = 0$ to 0.4). Differences in solution chemistry in these two systems are exemplified by the fact that silica gels exist in nature ([5]) and synthetic silica gels were first reported in the nineteenth century ([6]), however the first synthesis of a borate-based gel was reported in 1984 ([7]). Structural differences are demonstrated by the most commonly accepted models for the structures of the corresponding melt-prepared glasses : whereas v-SiO$_2$ is a 4-2 continuous random network ([8]), vitreous alkali-borates are composed of polyborate structural units giving rise to intermediate range order ([9]).

The following two sections discuss the structures of silicate and borate gels, respectively. We emphasize results obtained from experiments in which structural information is inferred from the chemical reactivity of network structures with water and alcohol. Structural information is discussed in terms of recent models of conventionally melted glasses to show how structural studies of gels provide insight into the structure of the amorphous state.

II. Dependence of chemical reactivity on the structure of gels : Defects in SiO$_2$

Structural origins of narrow bands in the Raman spectrum of vitreous silica (v-SiO$_2$) at 490 and 608 cm^{-1}, have provoked heated controversies in recent years ([10-14]). It is generally accepted that these bands are not predicted by continuous random network models of v-SiO$_2$ ([15]). Therefore structures responsible for the bands have been ascribed to defects, and the 490 and 608 cm^{-1} Raman bands have been labeled D1 and D2, respectively.

Depending on the synthesis conditions and thermal history, the relative intensities of the D1 and D2 bands in silicate gels may be dramatically enhanced compared to conventional v-SiO$_2$ ([16-18]) (see Fig. 1). In a recent review article we presented experimental evidence concerning the behavior of the defect bands in gels and concluded that all of the available evidence on gels supported Galeener's model in which the D1 and D2 bands are identified as the symmetric ring breathing modes of vibrationally decoupled 4- and 3- fold rings, respectively (cyclic tetra- and tri-siloxanes) ([13]). Since our review, several papers have been published which use the Raman evidence obtained from gels to support alternative structural models for D1 and D2 ([11,12,14]). We now review our former arguments and discuss additional experimental results in the context of these recently proposed models.

II.1. Behavior of Defects in Gels

Our combined results of Raman spectroscopy, differential scanning calorimetry (DSC), and thermal gravimetric analyses (TGA) performed on silica gels (synthesized with and without ^{18}O enrichment) are summarized as follows ([13,18]) : 1) The D1 and D2 vibrations in gels
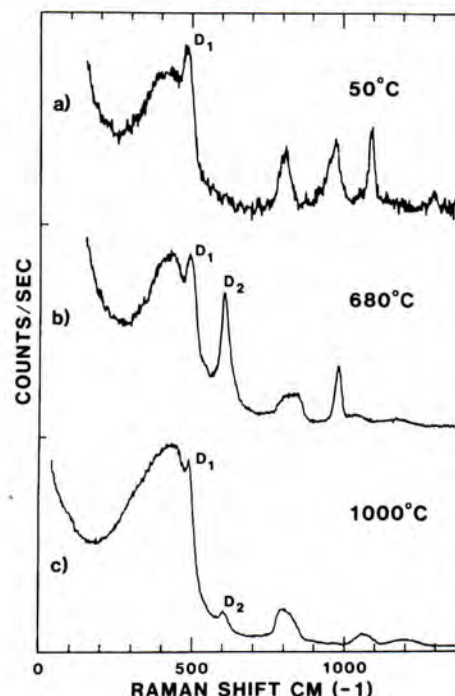

Fig. 1. — Raman Spectra of SiO$_2$ gels a) after desiccation at 50 °C; b) after heating to 680 °C according to : 1 °C/min to 350 °C (10 hr hold); 1 °C/min to 680 °C (2 hr hold); c) after densification at 1 000 °C. The densified gel spectrum (c) is essentially identical to conventional v-SiO$_2$.
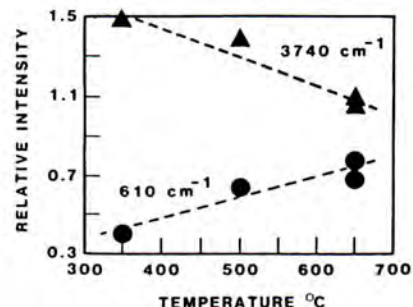

Fig. 2. — Integrated relative intensities of Raman bands at 610 cm^{-1} (D2) and 3 750 cm^{-1} (SiO-H stretching) during heating at 10 °C/min.

occur at the same frequencies as in conventional v-SiO$_2$, and, based on ^{18}O enrichment studies, both vibrations involve nearly pure oxygen motion. 2) The structure responsible for D1 is present in the air-dried xerogel (50 °C), and its concentration is only moderately affected by heating (Fig. 1). 3) The D2 structure is essentially absent in the dried xerogel. On heating it is present by 250 °C and its concentration increases significantly between 350 and 650 °C. Above 900 °C, where complete densification occurs via viscous sintering, the concentration of D2 decreases to a level comparable to that in conventional v-SiO$_2$ (Fig. 1). 4) In the temperature region 350-650 °C the relative intensity of D2 increases monotonically and the relative intensities of bands at 3 750 and 980 cm^{-1}, assigned to isolated vicinal SiO-H and Si-OH stretching vibrations, respectively, decrease monotonically (see Fig. 2). 5) In this same temperature region oxygen atoms originating as surface silanols can be incorporated in the structures responsible for both the D1 and D2 vibrations. This is demonstrated in Figure 3 which compares the frequencies of D1 and D2 formed by dehydrating silica gel surfaces with and without ^{18}O enrichment. The reduced frequencies of
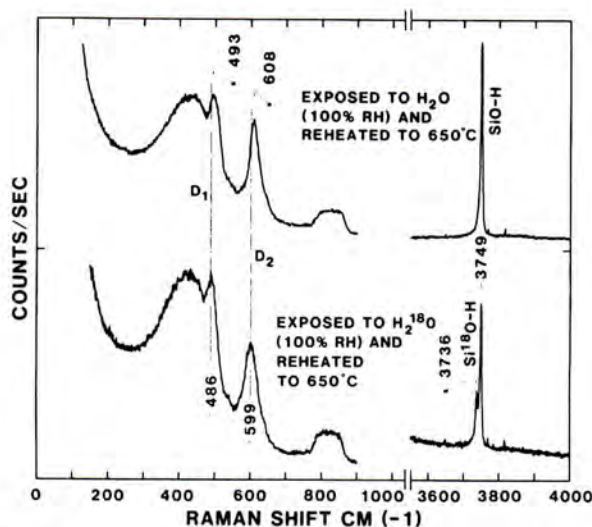
Fig. 3. — Raman spectra of porous gel-derived SiO_2 after an initial heat treatment to 650 °C and exposure to : a) H_2O (100 % RH) and reheated to 650 °C; b) $H_2{}^{18}O$ (100 % RH) and reheated to 650 °C.
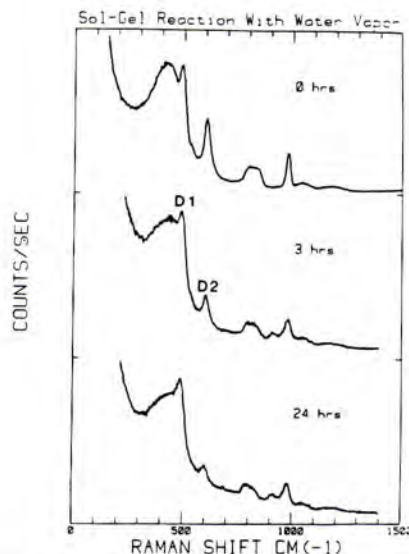

Fig. 4. — Raman spectra of porous gel-derived SiO_2 after an initial heat treatment to 650 °C followed by exposure to 100 % RH H_2O at 25 °C for the indicated times.

both D1 and D2 in the former case are evidence of ^{18}O incorporation. 6) Combined DSC and TGA experiments reveal that the net heat of formation of siloxane bonds in the temperature region 350-650 °C is significantly endothermic ($\Delta H_f \cong 19$ kcal/mole). 7) The D2 species is preferentially attacked by water vapor. Its concentration reduces to a level comparable to conventional v-SiO_2 in approximately eight hours at 100 % RH and 25 °C. Conversely, the D1 species is stable under these conditions (see Fig. 4).

The differing behaviors of the D1 and D2 defects show that, although both structures are able to form on the gel surface as products of condensation reactions involving isolated silanols, D1 and D2 are clearly two different defect species. The structure responsible for D1 is stable in solution and hence is evident in the dried product (xerogel). Conversely, the structure responsible for D2 is less stable in aqueous and/or alcoholic environments, and therefore is absent in the dried gel spectrum. D2 forms only by dehydroxylation of the silica

surface at intermediate temperatures and is metastable as evidenced by its positive heat of formation, its reduced concentration at high temperatures (where restructuring of the silica surface occurs) and its sensitivity to water vapor.

This evidence obtained on gels is consistent with Galeener's assignment of D1 and D2 to 4-fold and 3-fold rings, respectively ([15]). In gels both species can form by condensation reactions involving surface silanols :
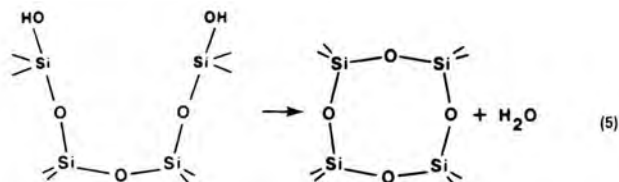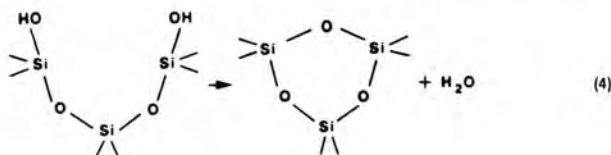
Based on the results of molecular orbital calculations ([17,20]) we expect the heat of formation of 4-fold rings to be weakly exothermic, whereas the heat of formation of 3-fold rings from unstrained precursors (Eq. 5) is calculated to be + 23 kcal/mole which is close to our experimentally-measured valued (19 kcal/mole). This positive ΔH_f largely reflects the energy required to reduce the Si-O-Si bond angle, ϕ, from its equilibrium value (viz. 144° observed in 4-fold and higher order rings) to 130° in the cyclic trisiloxane. The reduction in ϕ is also accompanied by charge transfer from silicon to oxygen, which makes the Si-O bond more ionic ([21]). Structure induced charge transfer with decreasing ϕ increases both the Lewis acidity of silicon and the Lewis basicity of oxygen. According to the strain enhanced fracture model of Michalske and Bunker ([22]), this in turn increases the susceptibility of siloxane bonds to dissociative reactions of the type :
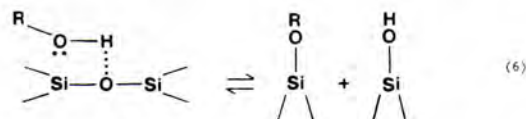
The observed sensitivity of D2 and the relative stability of D1 in alcohol and water environments appears to be completely consistent with the cyclic structural model. Further evidence in support of the cyclic model is derived from structural and environmental studies of model cyclic molecules ([13,23,24]). The frequencies of oxygen ring breathing modes were determined for cyclic di-, tri-, and tetra-siloxane molecules. The results are shown in Table 1 where they are compared to the observed frequencies of D1, D2, and oxygen ring breathing of the v-SiO_2 matrix (generally thought to consist of 5-fold and higher order rings). We observe a consistent scaling of frequency with decreasing ring size as predicted by theory ([19,20]). From this comparison it is logical to associate D1 with a cyclic tetrasiloxane species and D2 with a cyclic trisiloxane species.

Further comparisons may be made between the hydrolysis kinetics of model cyclic molecules and the D1 and D2 species. As indicated in Figure 4 the D1 species is stable in aqueous environments, whereas the D2

TABLE I

Si-O Stretching Frequencies of Siloxane Rings in Model Compounds and v-SiO$_2$

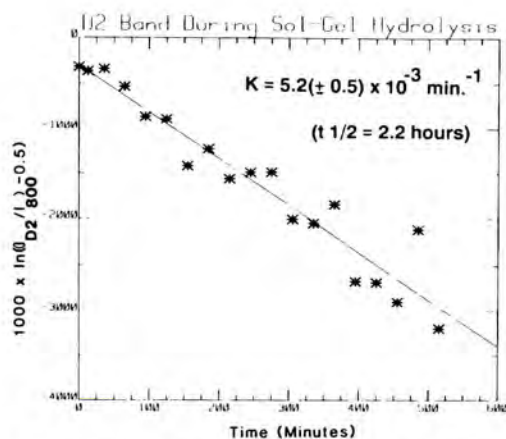| Functional Group	Source Material	Stretching Frequency (cm^{-1})
≥ 5-fold rings	v-SiO$_2$/SiO$_2$ gel	430
4-fold rings	Octamethyl cyclotetrasiloxane [25]	480
3-fold rings	Hexamethyl cyclotrisiloxane [24,25]	587
2-fold rings	Tetramesityl cyclodisiloxane [13,18]	873
D1	SiO$_2$ gel (Fig. 1)	490
D2	SiO$_2$ gel (Fig. 1)	608

Fig. 5. — First order kinetic plot for the hydrolysis of the D2 species at 25 °C and 100 % RH H$_2$O.

species undergoes gradual hydrolysis in 100 % RH (conditions under which water is condensed in the pores). After about eight hours the concentration of the D2 species is similar to that in conventional v-SiO$_2$, and for times greater than eight hours little further hydrolysis occurs. If we assume that the D2 species remaining after 8 hours are inaccessible to water vapor (the amount represented by D2 in the 24 hour spectrum in Fig. 4), a first-order kinetic plot (Fig. 5) indicates that D2 hydrolyzes with a first order rate constant of $5.2(\pm 0.5) \times 10^{-3}$ min^{-1} ($t_{1/2} = 2.2$ hours). By comparison hydrolysis investigations of model cyclic siloxane molecules in tetrahydrofuran solution at high water concentrations reveal that octamethylcyclotetrasiloxane is stable, and hexamethylcyclotrisiloxane hydrolyzes with a first order rate constant of $3.8 (\pm 0.4) \times 10^{-3}$ min^{-1} ($t_{1/2} = 3.0$ hours) [23,24]. Limited kinetic data suggest that cyclodisiloxanes hydrolyze at least four times faster than cyclotrisiloxanes [24]. Although the reactivity of small molecules in solution might be expected to differ from the reactivity of siloxane species constrained by a matrix, the similarity in hydrolysis kinetics is certainly supportive of the cyclic structural model for the D1 and D2 species.

Despite the substantial evidence which supports the cyclic model, Phillips [11,26] and Bertoluzza *et al.* [14] have used the observed behavior of D1 and D2 in gels to support alternative structural models. Phillips proposes that conventional v-SiO$_2$ is composed of paracrystalline clusters of cristobalite with diameters of about 6.0 to 7.5 nm. D1 and D2 represent the vibrations of siloxane species on (100)-like cristobalite cluster surfaces. Specifically, D1 is assigned to the transverse oxygen bending

mode of silanoperoxyl species, O$^\bullet_s$--O$^\bullet_s$, and D2 is assigned to the symmetric stretching vibrations of 4-fold rings which result from partial cluster fusion. Phillips uses the high concentrations of D1 and D2 in high surface area gels to support his model which localizes the defects on surfaces. In addition, the reported high reactivity of the defect species is used to verify his model in which the peroxyl bonds are claimed to be metastable. Several comments must be made regarding this cluster surface model. First, if conventional v-SiO$_2$ ($\rho = 2.21$ g/cm^3) were composed of 7.5 nm paracrystals of cristobalite ($\rho = 2.32$ g/cm^3), there are required 10^{19} paracrystals/cm^3 with a corresponding surface area of 808 m^2/g. According to this model conventional v-SiO$_2$ has an internal surface area which is roughly equivalent to the surface areas measured for gels (e.g., the 680 °C sample in Figure 1 has a measured BET surface area of 857 m^2/g). Thus the maximum increase in the concentration of defect species expected from the additional external surface area created by gel processing would be only a factor of approximately two. This cannot explain the $> 10 x$ increased relative intensity of D2 in gels dehydroxylated at intermediate temperatures (see Fig. 1). It should be noted that although D2 forms preferentially on silicate surfaces, high surface area alone does not guarantee a high concentration of D2. For example : the as-dried gel (S = 1 050 m^2/g) does not contain D2; the concentration of D2 increases by a factor of 2 in the temperature interval 350-650 °C where the surface area is decreased by over 20 %; and the concentration of D2 is reduced by 95 % on exposure to water vapor with less than 1 % change in surface area. Although the high surface area of gels and, e.g., fine silica powders [23] is necessary to observe enhanced concentrations of D2 compared to conventional vitreous silica, D2 is not characteristic of all silicate surfaces. D2 forms primarily by dehydroxylation of the silica surface at temperatures above about 200 °C where the hydroxyl coverage is about 6 OH/nm^2 [5]. Based on the calculated value of the heat of formation and measured values of the heat capacity and surface area, we estimate the maximum surface concentration of the D2 species to be about 3/nm^2. This relatively high concentration of D2 certainly suggests that the trisiloxane defect forms preferentially at the surface due to the decreased constraints of the matrix. However, once formed, the very high viscosity provided by the matrix preserves the defect until it is exposed to water or high temperature (reduced viscosity).

A second comment regarding the paracrystalline cluster model is that although the D1 band is assigned to metastable silanoperoxyl species, we observe that D2 is the environmentally sensitive species, and, conver-

sely, D1 is relatively unaffected by environmental exposure. Finally, D1 is assigned to a bending vibration of peroxide linkages. Previous Raman investigations of peroxide bonding in organo-silylperoxides ([27]) indicate that the only low frequency Raman active mode is a twist about the O—O axis (δ Si—O—O—Si) giving rise to two bands below 200 cm^{-1}. —O—O— stretching which has a greater Raman scattering cross section and hence should be more prominent than the associated twist occurs in the spectral region 900-1 000 cm^{-1} ([27]). In gels, bands in this region ($\sim$ 980 cm^{-1}) scale with those in the 3 600 3 750 cm^{-1} region and are assigned to Si-OH vibrations ([16]). During dehydroxylation of the silica gel surface, the relative intensity of the 980 cm^{-1} band decreases with respect to both D1 and D2. Thus, even if 980 cm^{-1} represented an O—O stretching band, silanoperoxyl bonding could not be associated with either defect species because the 980 cm^{-1} band and D1 and D2 exhibit opposite behavior (decreasing versus increasing relative intensities).

Bertoluzza et al. ([14]), agree that the D1 species is a cyclic tetrasiloxane but propose that the D2 defect involves partially broken Si—O bonds. Their hypothesis is based on the enhanced sensitivity of D2 to water vapor, its behavior with temperature (concentration increases then decreases), and investigations which indicate that alkali additions to silica gels (as sodium methoxide) greatly reduce the concentration of all defects.

If the D2 species did involve partially broken Si-O bonds, we should expect to observe a large concentration of paramagnetic centers using electron paramagnetic resonance (EPR) spectroscopy. However, EPR investigations of silica gels containing large concentrations of D2 revealed no paramagnetic centers prior to irradition ([28]). Furthermore, large dosages of gamma radiation produced large concentrations of unpaired spins but no apparent changes in the relative intensity of D2 (Fig. 6). With regard to the observation by Bertoluzza, et al., that D2 is reduced by alkali additions (both its maximum concentration and the temperature to which it is stable
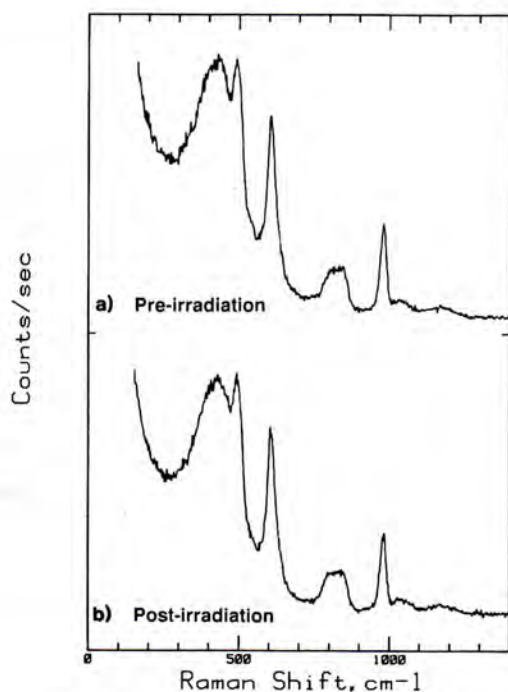
on heating) we can make the following comments. First the hydrolysis of the sodium methoxide precursor causes the pH of the silicate soluton to increase. Previous investigations by Bunker ([29]) indicate that both the surface area and defect concentration are reduced with increasing pH, because silicate bond rupture and reformation is promoted. This reconstructive process essentially allows the network to approach its equilibrium structure, i.e., low surface area and reduced concentrations of metastable species. Secondly, the viscosity of a pure silica system is drastically reduced by small concentrations of alkali. Hence the temperature at which the surface can begin to reconstruct (to eliminate defects) is reduced with increasing alkali concentration ([1-3]) as observed experimentally. Thus all the observations made by Bertoluzza et al. appear to be completely consistent with the cyclic structural model for the D1 and D2 defects.

III. Dependence of the structure of gels on chemical reactivity : Borate Gel Synthesis

The difference in solution chemistry of borates compared to silicates results from the fact that boron can exist either as trigonal coplanar with sp^2 hybridization or in tetrahedral coordination with sp^3 hybridization ([1]) :

$$\begin{array}{cc} \text{RO} & \\ \text{RO} \cdots \text{B} - \text{OR} & \qquad \text{RO} \\ \text{RO} & \end{array} \qquad (7)$$
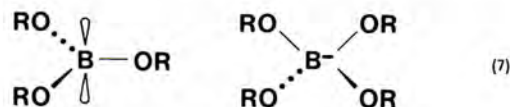
These differences in electronic structure dictate differences in the structures of stable solution species. For example in the trigonal configuration boron is electron deficient (and hence electrophilic) in the sense of the Lewis octet theory, making it susceptible to attack by water (hydrolysis) or alcohol (alcoholysis) according to the S$_N$2 mechanism :

$$\text{(8)}$$
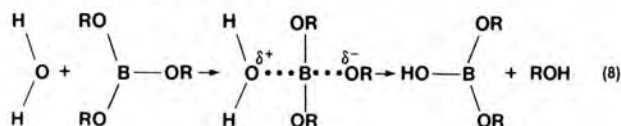
But because boron has no available low energy d orbitals, tetrahedrally coordinated boron cannot form the sp^3d transition state required for the S$_N$2 mechanism (Eq. 8). Therefore borate structures involving tetrahedral borons exhibit greater kinetic stability toward hydrolysis and alcoholysis and are prevalent solution species ([32]) (see Fig. 7).

With regard to ring formation, cyclic trimers appear to be the basic building block of the vast majority of polyborates. MO calculations of the cyclic borate trimer, H$_3$B$_3$O$_6$, reveal that the strain energy per BO bond is 1.7 kcal/mole ([33]). This value is 2.4 kcal/mole less positive than the strain energy per SiO bond calculated for cyclic trisiloxanes ([33]). Thus cyclic borate trimers are calculated to be 14.3 kcal/mole more stable than cyclic silicate

Fig. 6. — Raman spectra of porous gel-derived SiO$_2$: a) before irradiation and b) after 3 Mrad γ irradiation.

(Counts/sec — a) Pre-irradiation — b) Post-irradiation — Raman Shift, cm-1 — Ø 500 1000)

(1) Footnote : Tetrahedral borate anions (BO$_4^-$) are charge compensated by cations introduced, for example, as alkali or alkaline earth oxides. In crystalline and amorphous alkali borates the fraction of tetrahedral borons, N$_4$, increases with x as $x/(1-x)$ ([9]). ^{11}B NMR of lithium borate solutions showed that N$_4$ increased with x according to
$$N_4 = 0.1 + 0.4 \, x \; (^{30,31}).$$
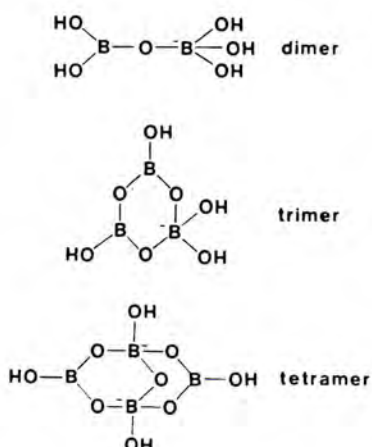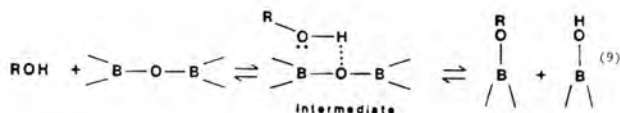
AQUEOUS BORATE SPECIES

Fig. 7. — Aqueous borate species : dimer, trimer and tetramer proposed by Edwards and Ross ([32]).

trimers. This difference in stability is reflected in the absence of D2 in as-dried silicate gels (Fig. 1) and in most silicate minerals, whereas cyclic borate trimers form the basic building blocks of virtually all borate minerals and glasses ([9]). Replacement of trigonal borons with tetrahedral borons should increase the kinetic stability of cyclic borate trimers. This is consistent with the observation that in aqueous solution the most prevalent borate polyanions are composed of various configurations of cyclic trimers containing one or two tetrahedral borons (see, e.g., Fig. 7). It is not understood, however, in what manner the introduction of tetrahedral borons affects overall ring strain.

While there have been numerous investigations of the structures of polyborate anions in aqueous solution, there have been no reports of gel formation. This suggests that although the primary structural units (see Fig. 7) are stable, these units do not in turn link together to form networks and hence gels. Therefore we suspect that gel formation in aqueous or alcoholic systems is limited by the stability of B-O-B bonds which link together primary structural units. This hypothesis is supported by investigations of v-B_2O_3 where B-O-B bonds linking trigonal borons contained in two separate primary units are observed to be much more susceptible to hydrolysis than trigonal B-O-B bonds contained within a single primary unit ([9]).

Based on hydrolysis mechanisms proposed to explain the aqueous corrosion of alkali borosilicate glasses ([29]), we expect the stability of B-O-B bonds towards dissociative reactions of the type :

$$ROH + \overset{}{\underset{}{>}}B-O-B\overset{}{\underset{}{<}} \rightleftharpoons \overset{}{\underset{}{>}}B\cdots\overset{O-H}{\underset{}{O}}\cdots B\overset{}{\underset{}{<}} \rightleftharpoons \overset{R}{\underset{}{O}}_{B} + \overset{H}{\underset{}{O}}_{B} \quad (9)$$

Intermediate

to decrease in the following order : [≡B-O-B≡] > [≡B-O-B=] > [=B-O-B=]. This ordering reflects the fact that boron cannot utilize sp^3d hybridization, and therefore nucleophilic attack by this mechanism is not possible for tetrahedral borons. In alkali borate systems containing both tetrahedral and trigonal borons we expect that the least stable bonds are B-O-B bonds linking trigonal borons contained in separate primary units. FTIR investigations of anhydrous and partially hydrolyzed crystalline lithium tetraborate support this
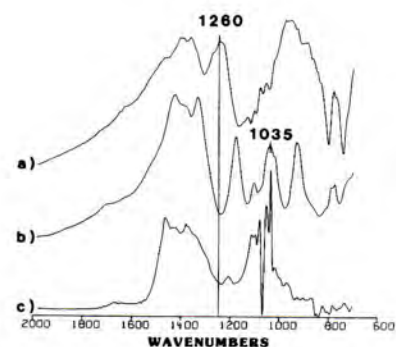

Fig. 8. — FTIR spectra of a) anhydrous crystalline lithium tetraborate, b) partially hydrolyzed lithium tetraborate, and c) difference spectrum, 120 hour aged sample spectrum minus 24 hour aged sample spectrum.
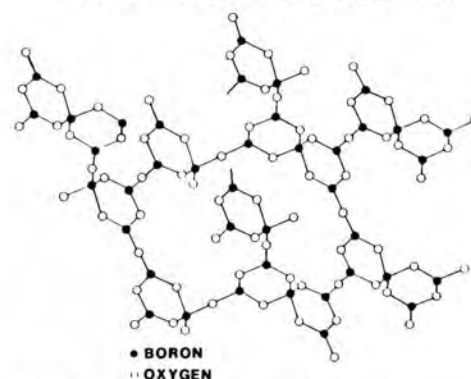
ANHYDROUS LITHIUM TETRABORATE

• BORON
∘ OXYGEN

Fig. 9. — A portion of the crystalline lithium tetraborate network showing linkages between primary units :
=B—O—B=   and   ≡B—O—B=

idea ([31]). The FTIR spectrum of anhydrous lithium tetraborate (Fig. 8a) exhibits a strong band at 1 260 cm^{-1} due to the asymmetric stretch of oxygens which link trigonal borons contained in different tetraborate structural units (Fig. 9). Exposure of this sample to 100 % RH for several hours results in a dramatic reduction in the relative intensity of the 1 260 cm^{-1} band (Fig. 8b). It is unlikely therefore that in alcohol/water solutions primary structural units could polymerize by forming B-O-B bonds linking trigonal borons contained within separate units. This criterion excludes pure B_2O_3 and establishes a minimum N_4 required for gelation.

In situ FTIR investigations of polymerization processes leading to gel formation in the lithium tetraborate system support the above hypotheses. The difference spectrum shown in Figure 8c represents molecular vibrations of the solution structures responsible for polymer growth and gelation. Comparisons with the spectra of anhydrous and partially hydrolyzed lithium tetraborate (Figs. 8a and 8b, respectively) clearly show the absence of the 1 260 cm^{-1} band in both the solution grown polyborates and the partially hydrolyzed crystalline sample. The environment of the trigonal borons (represented by the 1 300-1 500 cm^{-1} region) and the position and relative intensity of the 1 035 cm^{-1} band appear similar in both the gel and partially hydrolyzed crystal. Because of the greatly increased relative intensity of the 1 035 cm^{-1} band during polymer growth and the increased kinetic stability of borate bonds involving tetrahedral borons, we tentatively assign the 1 035 cm^{-1} band to the asymmetric B-O stretch of B-O-B bonds between primary units which link one trigonal and one

Tetraborate Network
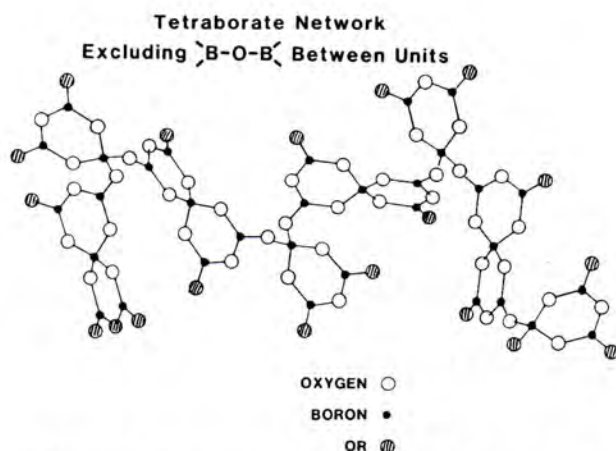### Excluding ⟩B-O-B⟨ Between Units

OXYGEN ○

BORON ●

OR ◕

Fig. 10. — Tetraborate network which excludes all =B—O—B= bonding between units.

tetrahedral boron. The strong bands at about 930 and 1 175 cm⁻¹, present only in the partially hydrolyzed lithium tetraborate spectrum, are assigned to B-O-H out of plane and in plane bending, respectively, on the basis of D_2O and $H_2^{18}O$ hydrolyses [31].

The above results may be used to arrive at a rational structural model for the borate gel. We begin with crystalline lithium tetraborate and eliminate all B-O-B bonds linking trigonal borons contained in different structural units. An infinite network is constructed by linking tetraborate units exclusively with kinetically stable B-O-B bonds involving one tetrahedral and one trigonal boron. This network preserves the tetraborate structural unit (and hence the environment of trigonal borons within units) and excludes all unstable trigonal =B-O-B= bonding between units. Non-bonded sites are terminated with alkoxide groups (Fig. 10).

Our borate gel formation model for aqueous and/or alcoholic environments limits gelation to systems in which there is a sufficient fraction of tetrahedral borons to form an infinite network which excludes trigonal B-O-B bonding between units. In alkali borate systems, $xR_2O \cdot (1-x) B_2O_3$, the minimum x which fulfills this criterion is $x = 0.2$ (maximum $N_4 = 0.25$). This corresponds to the minimum x in which gel formation was observed for lithium borate gels synthesized in a methoxyethanol/water solution. Replacing methoxyethanol with the cyclic ether, tetrahydrofuran, which contains no labile protons and hence is unable to react according to Eq. 9, extends the gel forming region to include all $x \geqslant 0.15$. Presumably, in THF trigonal B-O-B bonds between units exhibit increased stability, relaxing the critical N_4 requirement. Investigations are currently underway to determine whether or not structural differences (e.g., trigonal B-O-B bonding between units) exist between gels synthesized in alcoholic and THF environments.

IV. Summary

This paper summarizes how the structure of gels influences their chemical reactivity and vice versa. Gel structure evolves as the product of a complex series of hydrolysis and condensation steps. In solution the condensation products must be relatively stable with respect to hydrolysis or alcoholysis reactions in order to form gels. We demonstrated that the solution stability of silicate and borate structures is vastly different and depends primarily on the susceptibility of the silicon or boron atoms to nucleophilic attack. In silicate systems

the stability toward hydrolysis decreases with decreasing Si-O-Si bond angle (ø) as ø is reduced below about 145°. This is a result of the transfer of electron density from silicon to oxygen making silicon more acidic. Correspondingly, there is no evidence for cyclic trimers (ø ≅ 130°) or cyclic dimers (ø ≅ 90°) in the Raman spectra of the as-dried silica gels.

Compared to tetrahedral silicon, trigonal boron is significantly more electrophilic, which makes borate structures involving trigonal boron quite susceptible to hydrolysis. Interestingly, the most stable borate structures involving trigonal borons are those composed of cyclic trimers. Compared to cyclic trisiloxanes, the cyclic borate trimer is calculated to be significantly less strained. Presumably, this is a consequence of trigonal coplanar sp^2 versus tetrahedral sp^3 hybridization in boron and silicon, respectively. Alkali oxide additions to borate solutions cause boron to increase its coordination to four. Because boron has no low energy d orbitals, tetrahedral boron is not susceptible to hydrolysis via a S_N2 reaction. Thus, borate structures involving tetrahedral borons exhibit greater kinetic stability toward hydrolysis. B-O-B bonds linking primary structural units appear to be the "weakest link" in polyborate solution species. In alcohol/water solutions there is no evidence for trigonal B-O-B bonds between primary structural units. Gel formation occurs only when there is sufficient tetrahedral boron that bonding between primary units can occur exclusively as B-O-B (minimum N_4 equals 0.25). These constraints are mollified when alcohol is replaced with an aprotic solvent.

During gel densification at elevated temperatures, condensation reactions continue to occur. Above about 200 °C dehydroxylation of the silica surface results in large concentrations of cyclic trisiloxanes as evidenced by the intense Raman band at 608 cm⁻¹ (D2). Apparently, due to the lack of constraint by the matrix, trisiloxane ring formation is facile on the silica surface. Once formed however, these metastable species are stabilized by the high viscosity of the surrounding silica matrix. Under inert conditions cyclic trisiloxanes are prevalent on the silica surface until the temperature is sufficiently elevated (viscosity sufficiently reduced) that the surface is able to undergo reconstruction. Fully densified gels exhibit concentrations of cyclic trisiloxanes which are comparable to those in conventional v-SiO₂.

The consequences of having large concentrations of strained species on the silica surface are three-fold. First the reactivity of the surface toward environmental molecules which are able to undergo dissociative chemisorption is significantly enhanced. Compared to the estimated rate constant for the hydrolysis of unstrained siloxane bonds (estimated by extrapolation of the data in ref. 34) the rate of hydrolysis of cyclic trisiloxanes is greater by a factor of approximately 75. Second, the positive heat of formation of the strained species results in an effective increase in surface energy. Thus the formation of these species causes the porous gel to contract and conversely their elimination causes dilation [39]. Third, the redistribution of charge associated with the reduction in the Si-O-Si bond angle may influence catalysis on supported porous silica substrates.

Finally, we should emphasize that for temperatures below the conventional T_g space the structure of gels reflects a series of condensation steps. To further our understanding of gel formation and structure, we must thoroughly understand condensation mechanisms and the stability of condensation products in the synthesis medium. This paper demonstrates the benefit of ad-

dressing the structure of gel problem from both forward (condensation) and backward (dissolution) directions. This approach has provided significant evidence in support of the cyclic siloxane model for the Raman active defects D1 and D2, in v-SiO$_2$.

Acknowledgments

References

(1) C.J. Brinker and G.W. Scherer. — *J. Non-Cryst. Solids*, 1985, **70**, 301-322.

(2) C.J. Brinker, G.W. Scherer and E.P. Roth. — *J. Non-Cryst. Solids*, 1985, **72**, 345-368.

(3) G.W. Scherer, C.J. Brinker and E.P. Roth. — *J. Non-Cryst. Solids*, 1985, **72**, 369-389.

(4) G.W. Scherer. — Relaxation in Glass and Composites, (Wiley Interscience, NY) 1986.

(5) R.K. Iler. — *The Chemistry of Silica*, Wiley, NY, 1979.

(6) M. Ebelmen. — *Comptes Rend de L'Acad. des Sciences*, 1947, **25**, 854.

(7) N. Tohge, G.S. Moore and J.D. Mackenzie. — *J. Non-Cryst. Solids*, 1984, **63**, 95.

(8) W.H. Zachariasen. — *J. Chem. Phys.*, 1932, *54*, 3841.

(9) J. Krogh-Moe. — *J. Phys. Chem. Glasses*, 1965, **6**, 46.

(10) F.L. Galeener and A.C. Wright. — *Sol. State Comm.*, 1986, **57**, 677.

(11) J.C. Phillips. — *Phys. Rev. B*, 1986, **33**, 4443-4445.

(12) A. Chmel and G.M. Sochivkin. — *Sol. State Comm.*, 1986, **58**, 363-365.

(13) C.J. Brinker, D.R. Tallant, E.P. Roth and C.S. Ashley. — *Mat. Res. Soc. Symp. Proc.*, 1986, **61**, 387-411.

(14) A. Bertoluzza, C. Fagnano, M.A. Morelli, V. Gottardi, M. Guglielmi. — *J. Non-Cryst. Solids*, 1986, **82**, 127-136.

(15) F.L. Galeener. — In : *The Structure of Non-Crystalline Materials 1982*, eds : P.H. Gaskell, J.M. Parker and E.A. Davis, (Taylor & Francis, Ltd., London 1983).

(16) D.M. Krol and J.G. Van Lierop. — *J. Non-Cryst. Solids*, 1984, **63**, 131.

(17) V. Gottardi, M. Guglielmi, A. Bertoluzza, C. Fagnano, and M.A. Morelli. — *J. Non-Cryst. Solids*, 1984, **63**, 71.

(18) C. J. Brinker, D. R. Tallant, E.P. Roth and C. S. Ashley. — *J. Non-Cryst. Solids*, 1986, **82**, 117-126.

(19) T. Kudo and S. Nagase. — *J. Am. Chem. Soc.*, 1985, **107**, 2589.

(20) M. O'Keefe and G. V. Gibbs. — *J. Chem. Phys.*, 1984, **81**, 876.

(21) M. D. Newton and G. V. Gibbs. — *Phys. Chem. Mineral.*, 1980, **6**, 221.

(22) T. A. Michalske and B. C. Bunker. — *J. Appl. Phys.*, 1984, **56**, 2686-2693.

(23) D. R. Tallant, B. C. Bunker, C. J. Brinker and C. A. Balfe. — *Mat. Res. Soc. Symp. Proc.*, 1986, **73**, 261-268.

(24) C. A. Balfe, K. J. Ward, D. R. Tallant and S. L. Martinez. — *Mat. Res. Soc. Symp. Proc.*, 1986, **73**, 619-626.

(25) A. F. Smith and D. R. Anderson. — *Appl. Spect.*, 1984, **38**, 822.

(26) J. C. Phillips. — *Sol. St. Comm.* submitted.

(27) V. A. Simon and H. Arnold. — *J. Prakt. Chem.*, 1959, **4**, 241-255.

(28) C. J. Brinker and P. M. Lenahan. — Unpublished results.

(29) B. C. Bunker. — *Mat. Res. Soc. Symp. Proc.*, 1986, **73**, 49-56.

(30) C. J. Brinker, K. J. Ward, K. D. Keefer, E. Holupka, P. J. Bray and R. K. Pearson. — In *Aerogels*, Ed. J. Fricke, (Springer Verlag, Berlin, 1986), 387-411.

(31) C. J. Brinker, K. J. Ward, K. D. Keefer and E. Holupka. — *Mat. Res. Soc. Proc.*, 1986, **73**, 57-70.

(32) J. O. Edwards and V. Ross. — *J. Inorg. Nucl. Chem.*, 1960, **15**, 329.

(33) Z. G. Zhang, M. B. Boisen Jr., L. W. Finger and G. V. Gibbs. — *Am. Mineral*, 1985, **70**, 1238-1247.

(34) W. Stöber. — *Adv. Chem. Series*, 1967, *67*, 161.

(35) C. J. Brinker and S. T. Reed. — Unpublished results.